

Heterometallic Ion-Regulated Full-Color Gold Nanoclusters for Multicolor Bioimaging and Circularly Polarized Luminescence

Yaguang Yin[#], Gan Zhao[#], Fanfan Yu, Honglin Liu*

Joint Research Center for Food Derived Functional Factors and Synthetic Biology of IHM, Anhui Provincial International Science and Technology Cooperation Base for Major Metabolic Diseases and Nutritional Interventions, China Light Industry Key Laboratory of Meat Microbial Control and Utilization, School of Food and Biological Engineering, Engineering Research Center of Bio-process, Ministry of Education, Hefei University of Technology, Hefei 230601, P. R. China

[#] Yaguang Yin and Gan Zhao contributed equally to this work.

*Corresponding Author E-mail: liuhonglin@mail.ustc.edu.cn ; liuhonglin@hfut.edu.cn

Experimental Section

Materials

Chloroauric acid hydrate ($\text{HAuCl}_4 \cdot 4\text{H}_2\text{O}$), sodium hydroxide (NaOH), hydrochloric acid (HCl), magnesium chloride hexahydrate ($\text{MgCl}_2 \cdot 6\text{H}_2\text{O}$), silver nitrate (AgNO_3), methanol, ethanol, propan-2-ol (IPA), N,N-Dimethylformamide (DMF), dimethyl sulfoxide (DMSO), tetrahydrofuran (THF), dichloromethane (CH_2Cl_2) and sodium bicarbonate (NaHCO_3) were purchased from Sinopharm Chemical Reagent Co., Ltd. 4-amino-2-mercaptopyrimidine (AMP) and trifluoroacetic acid (TFA) were purchased from Aladdin Holdings Group Co., Ltd. Chromium(III) nitrate nonahydrate ($\text{Cr}(\text{NO}_3)_3 \cdot 9\text{H}_2\text{O}$) were achieved from Shanghai Macklin Biochemical Technology Co., Ltd. D-/L-Glutamic acid (D/L-Glu), octadecylamine (ODA), 1-(3-Dimethylaminopropyl)-3-ethylcarbodiimide hydro (EDC) and 1-Hydroxybenzotriazole (HOBT) were obtained from Shanghai yuanye Biotechnology Bureau Co., Ltd. All chemicals were used without further purification. Ultrapure Milli-Q water was used throughout all experiments.

Characterizations

UV-vis absorption spectra and fluorescence spectra were collected by a Shimadzu UV-2600 spectrometer and a F98 fluorospectrophotometer, respectively. Infrared spectra were measured using FT-IR Spectrometer (PerkinElmer Frontier). Photoluminescence lifetimes were measured by time-correlated single-photon counting (TCSPC) on a Horiba fluoromax spectrofluorometer. X-ray photoelectron spectra (XPS) were acquired on a Thermo ESCALAB 250 with $\text{Al K}\alpha$ ($h\nu=1486.6$ eV) as the excitation source. The transmission electron microscopy (TEM) image was recorded with a JEM-2100F field emission electron microscope at an accelerating voltage of 200 kV. Electrospray ionization mass spectrometry (ESI-MS) measurements were performed using a Waters UPLC H-class/XEVOG2-XS Qtof mass spectrometer from Waters Corporation, USA.

Co-assembled gel was characterized by Regulus 8230 high-resolution field-emission scanning electron microscopy (HRSEM). Circular dichroism (CD) was tested on a circular dichroism spectrometer JASCO-1700. The circularly polarized luminescent (CPL) spectra were recorded using a JASCO CPL-300 spectropolarimeter. CytoFLEX flow cytometry was used to collect data on apoptosis. Fluorescence images were obtained with a fluorescence microscope (Nikon Eclipse 80i, Japan).

Synthesis of full-color Au NCs

Synthesis of blue-emitting Au NCs (b-NCs): First, 50 μL of H_2O , HAuCl_4 (30 μL , 250 mM) and $\text{Cr}(\text{NO}_3)_3$ (500 μL , 0.1 M) were sequentially added to 900 μL AMP solution (25 mM), and then 20 μL of 1 M HCl solution was added. After rapid stirring (1000 rpm) for 12 h at room temperature (30°C), the reaction solution was centrifuged at 10,000 rpm for 6 min. The collected supernatant was purified overnight using a dialysis bag with a molecular weight cutoff of 500 Da and dispersed in an aqueous solution.

Synthesis of blue-emitting Au NCs (Cr-free): First, 550 μL of H_2O and HAuCl_4 (30 μL , 250 mM) were sequentially added to 900 μL AMP solution (25 mM), and then 20 μL of 1 M HCl solution was added. After rapid stirring (1000 rpm) for 12 h at room temperature (30°C), the reaction solution was centrifuged at 10,000 rpm for 6 min. The collected supernatant was purified overnight using a dialysis bag with a molecular weight cutoff of 500 Da and dispersed in an aqueous solution.

Synthesis of blue-emitting Au NCs (Au-free): First, 80 μL of H_2O and $\text{Cr}(\text{NO}_3)_3$ (500 μL , 0.1 M) were sequentially added to 900 μL AMP solution (25 mM), and then 20 μL of 1 M HCl solution was added. After rapid stirring (1000 rpm) for 12 h at room temperature (30°C), the reaction solution was centrifuged at 10,000 rpm for 6 min. The collected supernatant was purified overnight using a dialysis bag with a molecular weight cutoff of 500 Da and dispersed in an aqueous solution.

Synthesis of green-emitting Au NCs (g-NCs): Firstly, 5 μL of H_2O , HAuCl_4 (30 μL , 250 mM) and MgCl_2 (500 μL , 0.1 M) were sequentially added to 900 μL AMP solution (25 mM), and then 65 μL of 1 M NaOH solution was added. After rapid stirring (1000 rpm) for 4 h at room temperature (30°C), the reaction solution was centrifuged at 10,000 rpm for 6 min. The collected supernatant was purified overnight using a dialysis bag with a molecular weight cutoff of 500 Da and dispersed in an aqueous solution.

Synthesis of green-emitting Au NCs (Mg-free): Firstly, 505 μL of H_2O and HAuCl_4 (30 μL , 250 mM) were sequentially added to 900 μL AMP solution (25 mM), and then 65 μL of 1 M NaOH solution was added. After rapid stirring (1000 rpm) for 4 h at room temperature (30°C), the reaction solution was centrifuged at 10,000 rpm for 6 min. The collected supernatant was purified overnight using a dialysis bag with a molecular weight cutoff of 500 Da and dispersed in an aqueous solution.

Synthesis of green-emitting Au NCs (Au-free): Firstly, 35 μL of H_2O and MgCl_2 (500 μL , 0.1 M) were sequentially added to 900 μL AMP solution (25 mM), and then 65 μL of 1 M NaOH solution was added. After rapid stirring (1000 rpm) for 4 h at room temperature (30°C), the reaction

solution was centrifuged at 10,000 rpm for 6 min. The collected supernatant was purified overnight using a dialysis bag with a molecular weight cutoff of 500 Da and dispersed in an aqueous solution.

Synthesis of red-emitting Au NCs (r-NCs): Firstly, 350 μL of H_2O , HAuCl_4 (30 μL , 250 mM) and AgNO_3 (200 μL , 0.1 M) were sequentially added to 900 μL AMP solution (25 mM), and then 20 μL of 1 M NaOH solution was added. After rapid stirring (1000 rpm) for 12 h at room temperature (30°C), the reaction solution was centrifuged at 10,000 rpm for 6 min and the collected precipitate was dispersed in DMSO solution.

Synthesis of red-emitting Au NCs (Ag-free): Firstly, 550 μL of H_2O and HAuCl_4 (30 μL , 250 mM) were sequentially added to 900 μL AMP solution (25 mM), and then 20 μL of 1 M NaOH solution was added. After rapid stirring (1000 rpm) for 12 h at room temperature (30°C), the reaction solution was centrifuged at 10,000 rpm for 6 min and the collected precipitate was dispersed in DMSO solution.

Synthesis of red-emitting Au NCs (r-NCs): Firstly, 380 μL of H_2O and AgNO_3 (200 μL , 0.1 M) were sequentially added to 900 μL AMP solution (25 mM), and then 20 μL of 1 M NaOH solution was added. After rapid stirring (1000 rpm) for 12 h at room temperature (30°C), the reaction solution was centrifuged at 10,000 rpm for 6 min and the collected precipitate was dispersed in DMSO solution.

Synthesis of co-assembled gels

Synthesis of chiral gelators (LGAm/DGAm)¹: 0.1235 g L/D-Glu, 0.2695 g ODA, 0.201 g EDC and 0.1485 g HOBT were accurately weighed, followed by the addition of 10 mL of CH_2Cl_2 and stirring for 72 h. The white precipitate obtained by diafiltration was dissolved with THF, and then white floccule appeared by addition of water, and tiny white solids were obtained by diafiltration again. Subsequently, according to the ratio of 3.575 g of white solid, 50 mL of CH_2Cl_2 and 8 mL of TFA, stirring for three hours, and finally rotary evaporation of the stirred liquid with THF to dissolve the solid. Finally saturated NaHCO_3 was added and the white suspension was filtered to obtain gel powder which was dried for further use.

Synthesis of co-Assembled gels: The co-assembled gels were prepared by incorporating the synthesized gold nanoclusters (b-NCs, g-NCs, r-NCs) into the chiral gel matrices (LGAm or DGAm) using appropriate solvents and conditions. All final gels were uniformly coated onto solid quartz slides for fluorescence and circularly polarized luminescence (CPL) spectral measurements.

LGAm/b-NCs Gel: LGAm gel powder (20 mg) was mixed with ethanol (900 μ L) and the blue-emitting Au NCs solution (b-NCs, 100 μ L). The mixture was heated to ensure complete dissolution and mixing, then cooled to room temperature to form a white gel.

DGAm/b-NCs Gel: Prepared identically to LGAm/b-NCs, but using DGAm gel powder instead of LGAm.

LGAm/g-NCs Gel: LGAm gel powder (20 mg) was mixed with ethanol (900 μ L), the green-emitting Au NCs solution (g-NCs, 100 μ L), and a small quantity of silver ions (Ag^+). The mixture was heated to ensure complete dissolution and mixing, then cooled to room temperature to form a yellow gel.

DGAm/g-NCs Gel: Prepared identically to LGAm/g-NCs, but using DGAm gel powder instead of LGAm.

LGAm/r-NCs Gel: The red-emitting Au NCs (r-NCs) were dissolved in methanol (1 mL). LGAm gel powder (20 mg) was added to this solution. The mixture was heated to ensure complete dissolution and mixing, then cooled to room temperature to form a brown gel.

DGAm/r-NCs Gel: Prepared identically to LGAm/r-NCs, but using DGAm gel powder instead of LGAm.

Cell recovery and culture

Frozen HeLa cells stored at -80°C were rapidly thawed by gentle agitation in a 37°C water bath until the freezing medium within the cryovials was completely liquefied. The thawed cell suspension was then immediately transferred to a sterile biological safety cabinet. The suspension was diluted with pre-warmed complete culture medium supplemented with 10% fetal bovine serum. Cells were pelleted by centrifugation at 1,000 rpm for 5 minutes. The supernatant was carefully discarded, and the cell pellet was resuspended in fresh, pre-warmed culture medium. The resuspended cells were then transferred to appropriate cell culture flasks and incubated at 37°C in a humidified atmosphere containing 5% CO_2 for expansion and subsequent experimental use.

Cell apoptosis assay

Apoptosis was assessed using the Annexin V-FITC Apoptosis Detection Kit according to the manufacturer's protocol. Briefly, HeLa cells were incubated with b-NCs, g-NCs, or r-NCs (100 $\mu\text{g/mL}$) for 24 hours. Subsequently, the cells were washed twice with PBS buffer solution. Adherent cells were detached by incubation with 1 mL of trypsin solution at 37°C for approximately 2-3

minutes, followed by quenching with complete culture medium. The cell suspension was centrifuged at 1,000 rpm for 5 minutes to pellet the cells. The cell pellet was then washed twice by resuspension in 500 μ L of PBS buffer followed by centrifugation. After the final wash, cells were resuspended in 500 μ L of Annexin V Binding Buffer. Annexin V-FITC (5 μ L) and propidium iodide (5 μ L) were added to the cell suspension. The mixture was gently vortexed and incubated for 10 minutes on ice in the dark. Apoptotic cells were quantified immediately by flow cytometry.

ROS detection

Intracellular ROS levels were detected using the fluorescent probe 2',7'-dichlorodihydrofluorescein diacetate (DCFH-DA). HeLa cells seeded in six-well plates were incubated with b-NCs, g-NCs, or r-NCs (50 μ g/mL) for 24 hours. Following incubation, cells were gently washed twice with pre-warmed PBS buffer solution.

Positive control: Concurrently, a separate group of cells was treated with Rosup reagent (a ROS inducer) for 30 minutes at 37°C in a 5% CO₂ atmosphere to establish the positive control group. These cells were also washed twice with PBS after treatment.

Experimental groups: Cells from both the NC-treated experimental groups and the Rosup-treated positive control group were then incubated with DCFH-DA (10 μ M final concentration, diluted in serum-free medium) for 30 minutes at 37°C in the dark.

Cell harvest: After incubation, cells were washed three times with pre-warmed serum-free medium to remove excess probe. After washed with medium for three times, the cells were digested by trypsin, centrifuged, and resuspended in PBS.

Flow cytometry analysis: The fluorescence intensity of the oxidized product, 2',7'-dichlorofluorescein, within the cells was measured immediately using flow cytometry, with excitation at 488 nm and emission detection at 525 nm.

Cell imaging

Fluorescence microscopy was utilized to visualize the cellular uptake and intracellular distribution of the synthesized gold nanoclusters in HeLa cells. Cells were seeded onto glass-bottom culture dishes or coverslips and allowed to adhere overnight. The adherent cells were then incubated with b-NCs, g-NCs, or r-NCs (50 μ g/mL) in complete culture medium at 37°C under a 5% CO₂ atmosphere for 2 hours. Following incubation, the cells were gently washed three times with pre-warmed PBS buffer solution to remove any unbound nanoclusters. and fluorescence images were

subsequently captured by fluorescence microscopy.

Preparation and analysis of CPL encryption matrix

The circularly polarized luminescence (CPL) encryption matrix was fabricated using the six synthesized chiral co-assembled gels (LGAm/b-NCs, DGAm/b-NCs, LGAm/g-NCs, DGAm/g-NCs, LGAm/r-NCs, DGAm/r-NCs). Approximately 150 μL of each gel was precisely dispensed onto discrete, predefined regions of a clean circular glass slide. The deposited gels were allowed to undergo complete gelation at room temperature. The solidified gel array slide was then mounted onto a rigid support to form the integrated encryption platform.

Decryption procedure:

Level-1 Decoding (Fluorescence Emission): The encrypted matrix was illuminated under 365 nm UV light. The emitted fluorescence color (blue, green, or red) from each gel spot was visually identified and digitally encoded according to a predefined scheme: blue = 1, green = 2, red = 3. This assignment generated the primary decryption matrix based on fluorescence color.

Level-2 Decoding (CPL Handedness): The circularly polarized luminescence characteristics of each spot were analyzed. The emitted CPL was converted to linearly polarized light using a quarter-wave plate. This linear polarization was then interrogated using a right-handed linear polarizer. Spots exhibiting right-handed CPL were assigned a value of +1, while those exhibiting left-handed CPL were assigned -1. This yielded the secondary decryption matrix based on the chirality of the emitted light.

Intensity quantification: In parallel, the mean fluorescence intensity for each gel spot within the array was quantified using ImageJ software.

The final decrypted message was obtained by computationally correlating the Level-2 matrix (chirality assignments) with the predetermined reference decryption key, potentially incorporating the quantified intensity data for enhanced security.

Computational Methods

All quantum chemical calculations were performed using the ORCA software package. Geometry optimizations were carried out with the BLYP-D3(BJ) functional in combination with Grimme's D3(BJ) dispersion correction and the def2-TZVP basis set. The RI approximation with the def2/J auxiliary basis was employed to accelerate computations. Frequency analyses were conducted to confirm that all optimized structures correspond to true minima with no imaginary

frequencies. Solvent effects were considered using the SMD implicit solvation model with water as the solvent. The Au cluster models were constructed with C₄H₄N₃S ligands, bridged by heterometal ions (Cr, Mg or Ag), while possible interligand N \cdots H hydrogen bonds were also included. The initial geometries were generated based on literature-reported bond lengths, followed by pre-optimization using GFN2-xTB and subsequent refinement at the density functional theory (DFT) level. Frontier orbital energies obtained from DFT were used to determine the HOMO, LUMO, and HOMO–LUMO energy gaps.

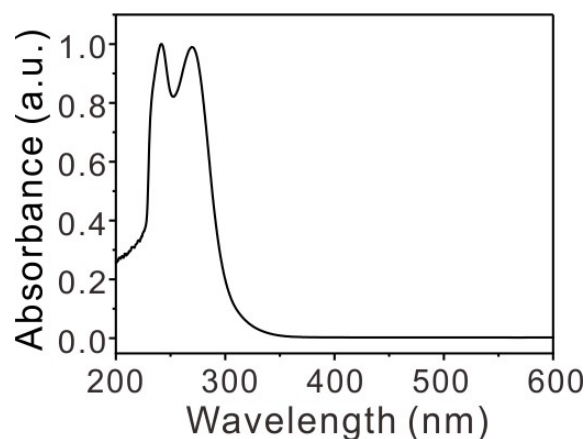


Figure S1. UV-vis absorption spectrum of the 4-amino-2-mercaptopyrimidine ligand in aqueous solution.

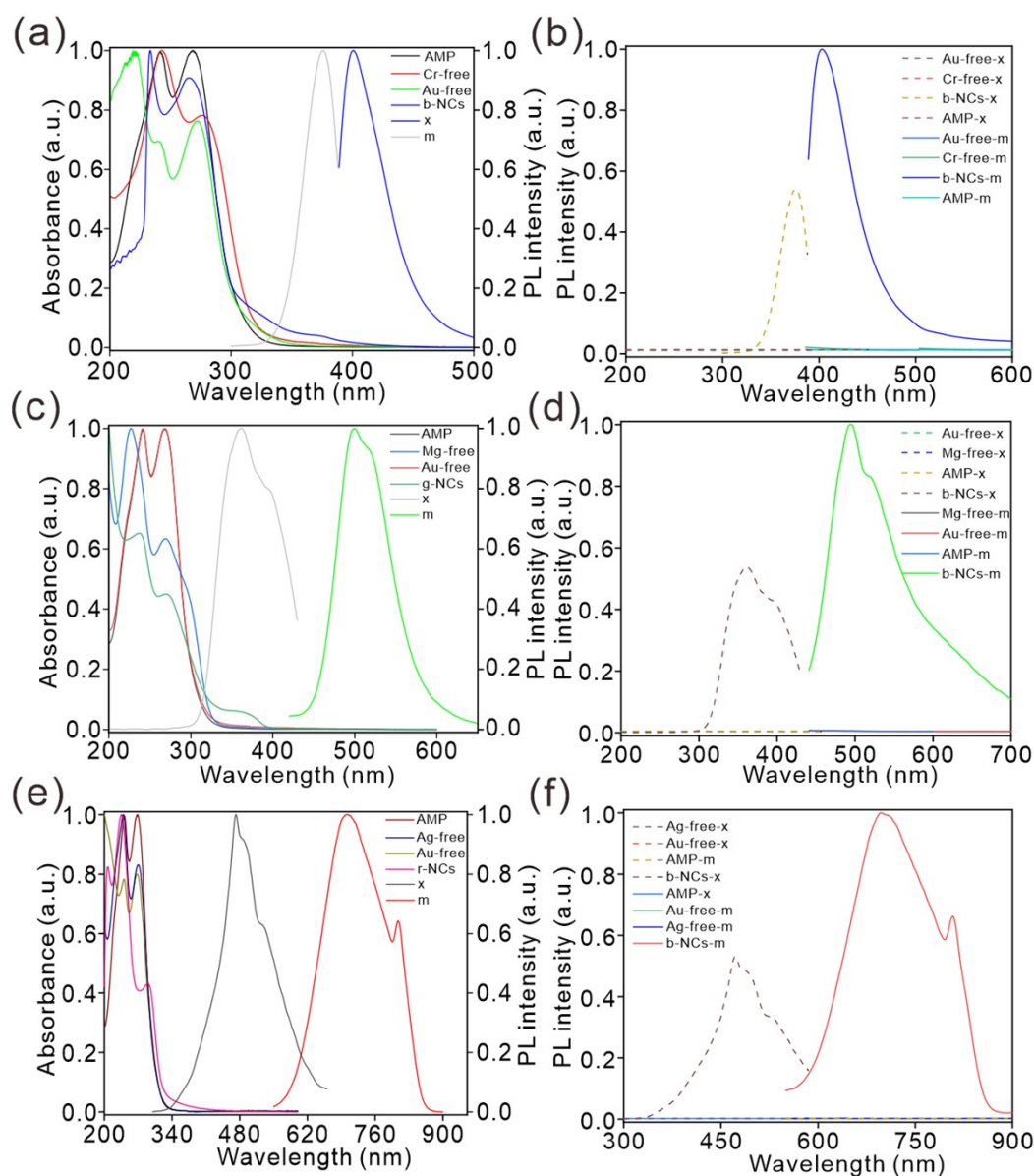


Figure S2. UV–vis absorption spectra of nanoclusters at different intermediate states together with excitation and emission spectra for comparison: (a) b-NCs, (c) g-NCs, and (e) r-NCs. Corresponding excitation and emission spectra of nanoclusters at different intermediate states: (b) b-NCs, (d) g-NCs, and (f) r-NCs. (x: Excitation wavelength, m: Emission wavelength)

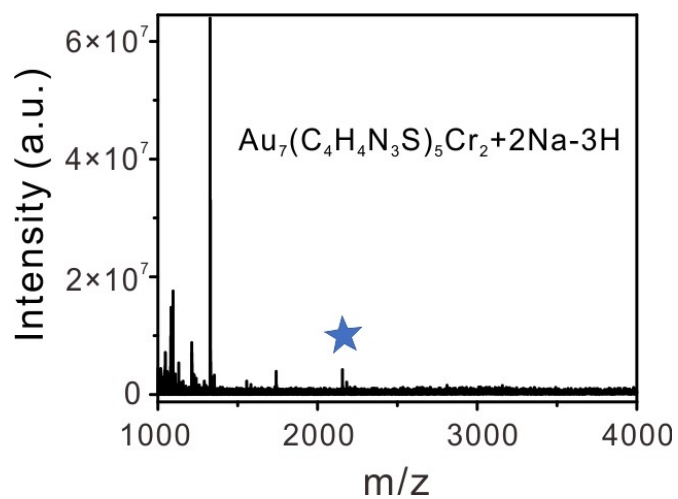


Figure S3. Electrospray ionization mass spectrometry (ESI-MS) spectrum of blue-emitting gold nanoclusters ($m/z=2156$).

Table S1. Strong fragment peaks of compound b-NCs and their assignments

Molecular weight	Chemical formula
1092	$[\text{Au}_4(\text{AMP})_2\text{Cr}]$
1212	$[\text{Au}_4(\text{AMP})_2\text{Na}_2]$
1331	$[\text{Au}_6(\text{AMP})_1\text{Na}]$
1738	$[\text{Au}_6(\text{AMP})_4\text{Cr}]$

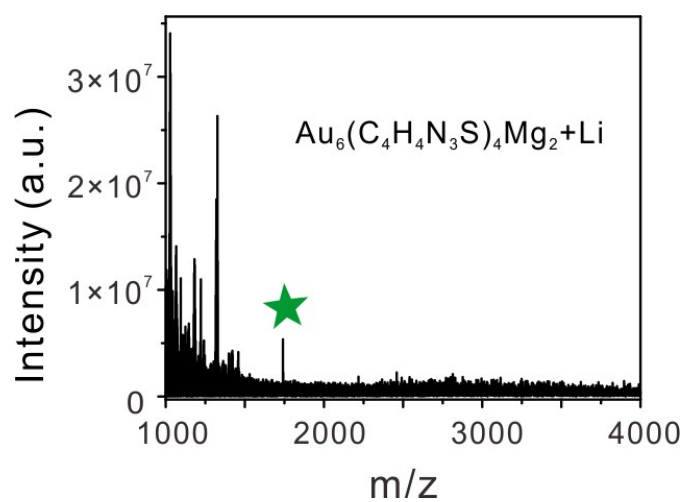


Figure S4. ESI-MS spectrum of green-emitting gold nanoclusters ($m/z=1741$).

Table S2. Strong fragment peaks of compound g-NCs and their assignments

Molecular weight	Chemical formula
1088	$[\text{Au}_4(\text{AMP})_2\text{Mg}_2]$
1182	$[\text{Au}_6]$
1332	$[\text{Au}_6(\text{AMP})\text{Mg}]$
1411	$[\text{Au}_5(\text{AMP})_3\text{Mg}_2]$

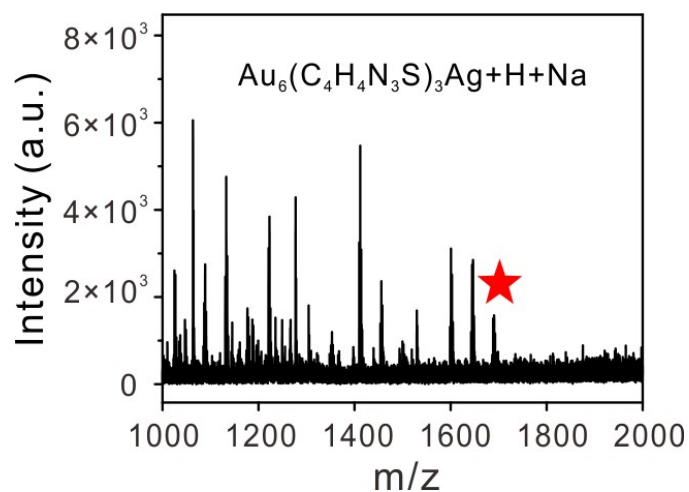


Figure S5. ESI-MS spectrum of red-emitting gold nanoclusters ($m/z=1691$).

Table S3. Strong fragment peaks of compound r-NCs and their assignments

Molecular weight	Chemical formula
1021	$[\text{Au}_4(\text{AMP})\text{Ag}]$
1134	$[\text{Au}_5(\text{AMP})\text{Na}]$
1273	$[\text{Au}_4(\text{AMP})_3\text{Ag}]$
1541	$[\text{Au}_6(\text{AMP})_2\text{Ag}]$

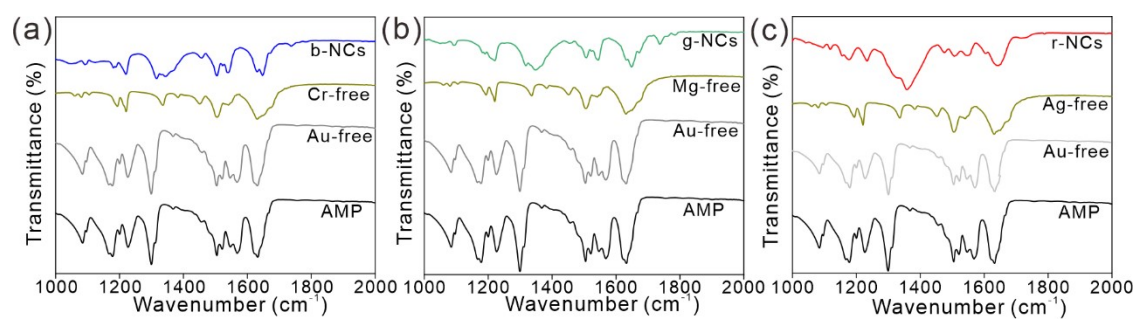


Figure S6. FTIR spectrum of (a) b-NCs, Cr-free, Au-free and AMP; (b) g-NCs, Mg-free, Au-free and AMP; (c) r-NCs, Ag-free, Au-free and AMP; respectively.

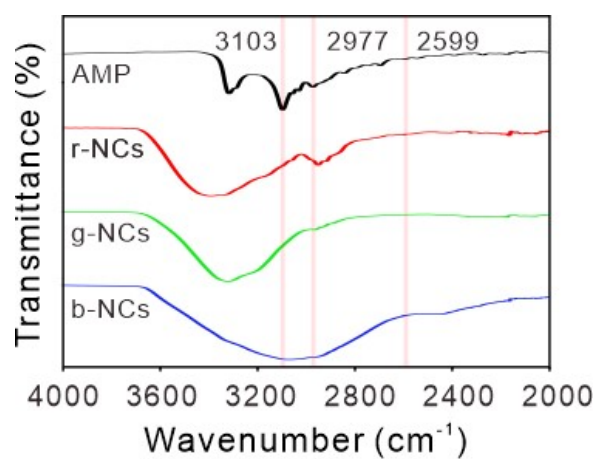


Figure S7. Fourier-transform infrared spectra of AMP ligand and heterometallic Au nanoclusters (b-NCs, g-NCs, r-NCs) recorded in transmission mode.

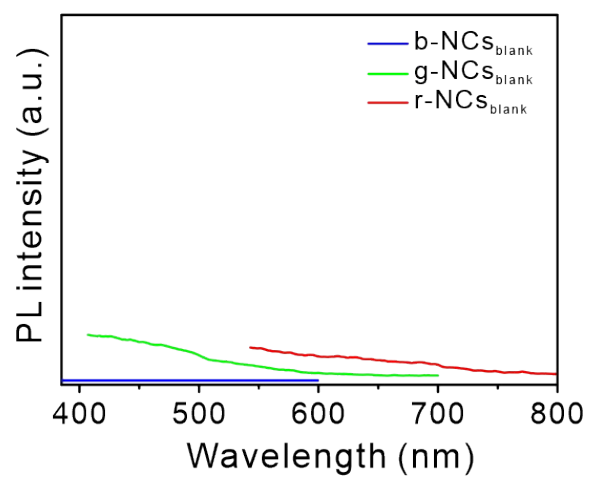


Figure S8. Fluorescence spectra of three Au NCs in the absence of heterogeneous metal ions.

Table S4. Key atomic interactions and corresponding bond lengths in the b-NCs cluster

Main interacting atom pairs	bond lengths (Å)	Main interacting atom pairs	bond lengths (Å)	Main interacting atom pairs	bond lengths (Å)
Au1-Au2	2.853	Au1-Au3	2.759	Au1-Au4	2.783
Au1-Au5	2.854	Au1-Au7	2.791	Au2-Au5	2.706
Au2-Au3	2.924	Au3-Au5	2.947	Au3-Au6	2.867
Au1-Au6	2.711	Cr17-S5	2.369	Cr17-S4	2.386
Cr9-S3	2.403	Cr9-S2	2.403	Au5-S5	2.447
Au4-S2	2.474	Au7-S4	2.455	Au2-S3	2.449

Table S5. Key atomic interactions and corresponding bond lengths in the g-NCs cluster

Main interacting atom pairs	bond lengths (Å)	Main interacting atom pairs	bond lengths (Å)	Main interacting atom pairs	bond lengths (Å)
Au6-Au2	2.687	Au6-Au3	2.712	Au6-Au4	2.716
Au6-Au5	2.739	Au6-Au1	2.974	Au2-Au3	2.741
Au4-Au5	2.670	Au3-S4	2.372	Au4-S3	2.438
Au5-S1	2.452	Au2-S2	2.454	Mg2-S3	2.714
Mg1-S1	2.638	Mg1-S2	2.638	Mg2-N11	2.112
Mg2-N8	2.134	Mg1-N5	2.094	Mg1-N2	2.098

Table S6. Key atomic interactions and corresponding bond lengths in the r-NCs cluster

Main interacting atom pairs	bond lengths (Å)	Main interacting atom pairs	bond lengths (Å)	Main interacting atom pairs	bond lengths (Å)
Au1-Au2	2.782	Au1-Au3	2.803	Au1-Au4	2.717
Au1-Au5	2.930	Au1-Ag1	2.783	Au2-Au5	2.629
Ag1-Au5	2.838	Ag1-Au4	2.839	Au3-Au4	2.677
Au6-Au3	3.170	Au6-S1	2.336	Au6-S3	2.372
Ag1-S2	2.415				

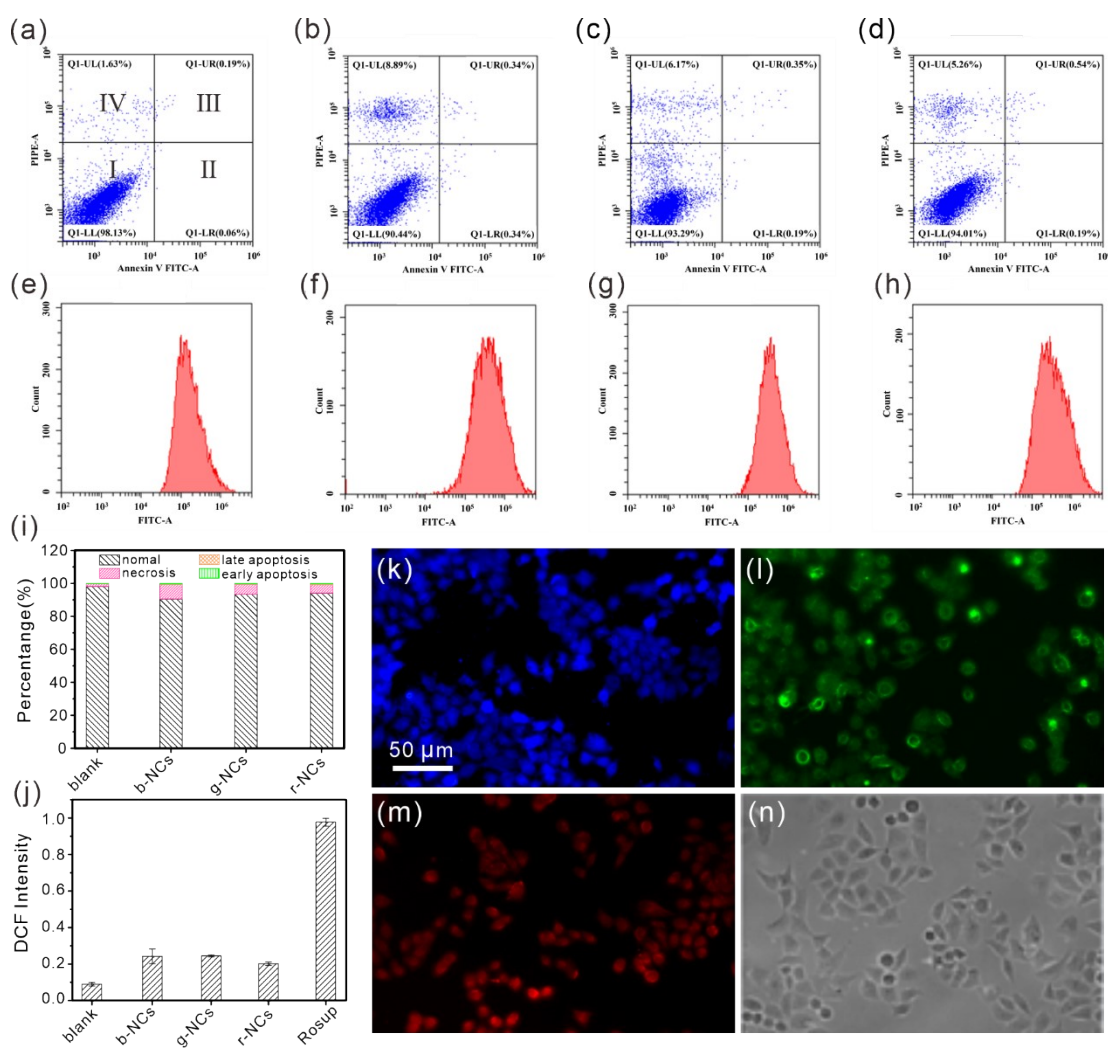


Figure S9. Cytotoxicity and cellular uptake analysis of heterometallic Au nanoclusters in HeLa cells. (a) Flow cytometry dot plots of Annexin V-FITC/PI staining for untreated control cells. (b-d) Apoptosis assay for cells treated for 24 h with 100 μ g/mL of (b) b-NCs, (c) g-NCs, and (d) r-NCs. (e) ROS-positive control. (f-h) Intracellular ROS detection after 24 h treatment with 100 μ g/mL of (f) b-NCs, (g) g-NCs, and (h) r-NCs. (i,j) Quantitative analysis of (i) apoptotic cells and (j) ROS-positive cells. (k-m) Fluorescence microscopy images showing cellular uptake after 2 h incubation with 50 μ g/mL of (k) b-NCs, (l) g-NCs, and (m) r-NCs. (n) Corresponding bright-field image of cells incubated with b-NCs (50 μ g/mL).

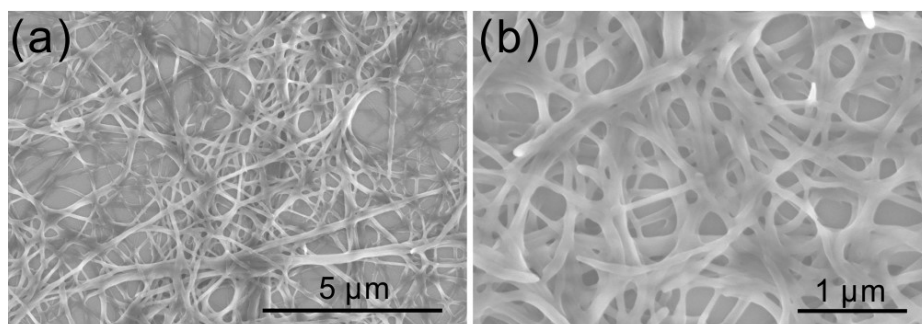


Figure S10. SEM images of pure LGAm gel in water/ethanol solvent mixture at different magnifications.

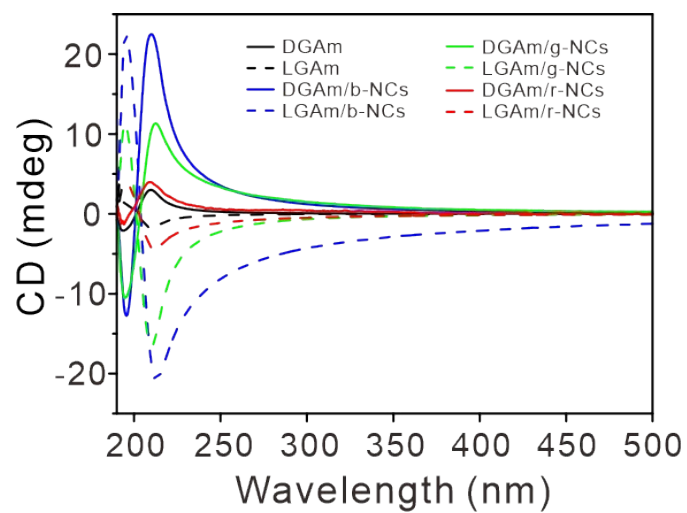


Figure S11. CD spectra of pure gels and three co-assembled gels.

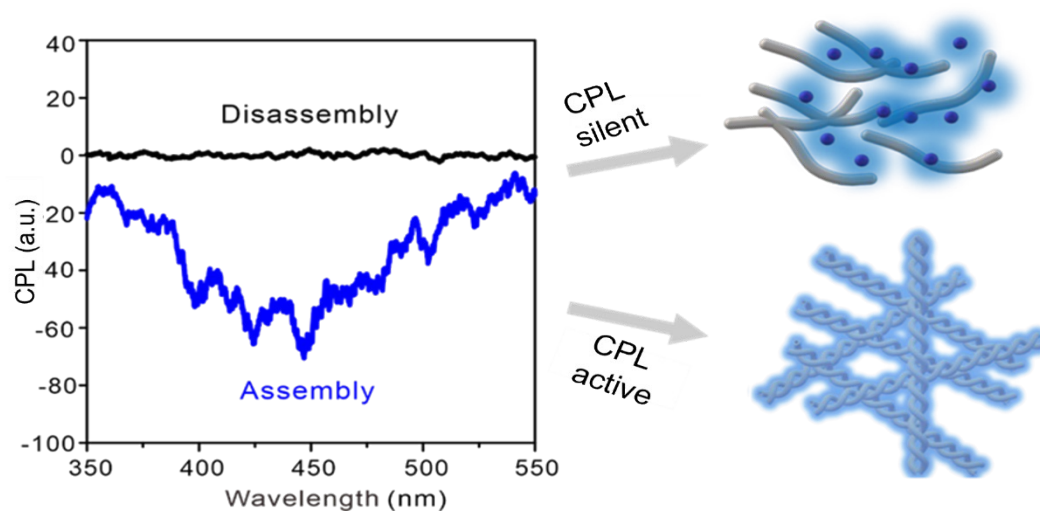


Figure S12. Principle of co-assembled gel CPL.

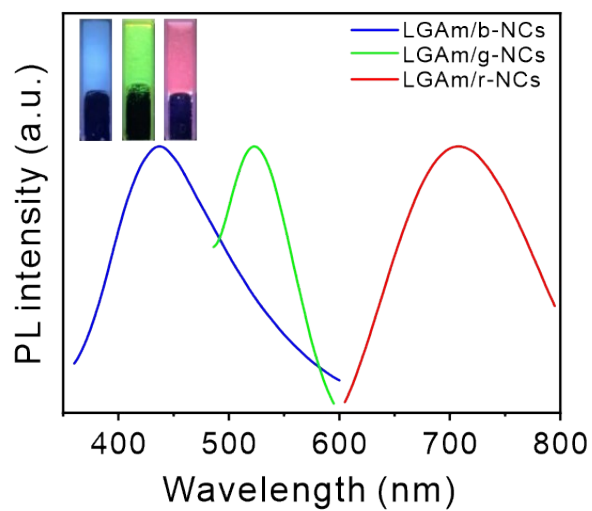


Figure S13. Solid-state fluorescence spectra of three chiral co-assembled gels: LGAm/b-NCs (blue line), LGAm/g-NCs (green line), and LGAm/r-NCs (red line). Inset: Digital photographs of the corresponding gels under 365 nm UV illumination, exhibiting blue, green, and red emission respectively.

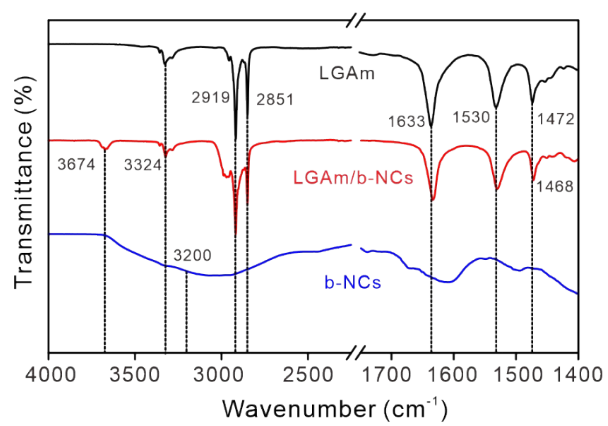


Figure S14. FTIR spectrum of LGAm, LGAm/b-NCs and b-NCs, respectively.

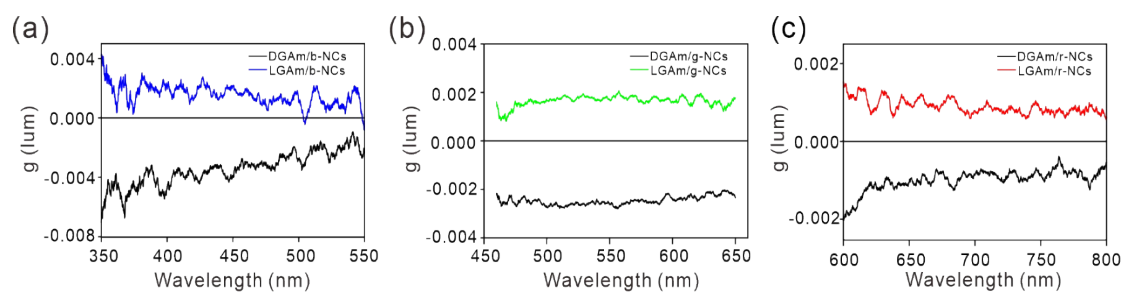


Figure S15. Circularly polarized luminescence (CPL) dissymmetry factor (g_{lum}) spectra of the chiral co-assembled gels: (a) LGAm/b-NCs and DGAm/b-NCs, (b) LGAm/g-NCs and DGAm/g-NCs, (c) LGAm/r-NCs and DGAm/r-NCs. The g -factor values quantify the degree of circular polarization in emitted light.

References:

1. Zhu, X.; Li, Y.; Duan, P.; Liu, M., Self-Assembled Ultralong Chiral Nanotubes and Tuning of Their Chirality Through the Mixing of Enantiomeric Components. *Chemistry-a European Journal*, 2010, 16 (27), 8034-8040.